Characteristic Impedance of Microshield Lines with Arbitrary Shield Cross Section

Jean-Fu Kiang

***Abstract*—A generalized potential-matching method incorporating reflection matrices is developed to calculate the capacitance of microshield lines with trapezoidal, circular, and V-shaped shields. Both completely shielded and half-shielded lines are analyzed. The effects of membrane thickness, strip width, and gapwidth on the characteristic impedance are studied.**

***Index Terms*— Capacitance, layered medium, microshield lines, potential-matching, reflection matrix.**

I. Introduction

A microshield line is a metal strip completely or partially enclosed within a cavity, and is supported mechanically by a thin membrane [1], [2]. The TEM mode is the dominant mode in such structures, and the membrane is supposed to incur as little dispersion as possible to the frequency response of the microshield lines. The shield serves to isolate the line from its neighboring circuits; hence, reducing or eliminating coupling, crosstalk, and parasitic substrate modes which may otherwise exist. The shield may have shapes other than rectangular due to material properties or processes. Hence, conventional mode-matching techniques applicable to layered medium enclosed by two straight boundaries cannot be applied to study the propagation properties of such lines [3].

If the shield boundary consists of straight line segments, conformal mapping using Schwartz–Christoffel transformation can be applied to obtain a closed-form expression involving elliptic integrals [4]–[6]. However, this approach cannot be applied if membrane exists inside the shield, as shown in Fig. 1. For microstrips embedded in a multilayered medium with layer interfaces conformal to concentric circles or confocal ellipses, the problem can be transformed to another one with flat microstrips embedded in a multilayered rectilinear medium [7].

The method of moments in the spatial domain can also be applied to obtain the capacitance of the microshield line. In [8], coupled strips with V-shaped lower shields have been analyzed. If layered medium inside the cavity is considered, the polarization charge at the interfaces between layers are used as unknowns to obtain the capacitance [9].

In this paper, we will develop a generalized potential-matching method to calculate the capacitance of microshield lines in which the shield is of arbitrary cross section and contains layered medium. Methodologically, it is similar to the full-wave field-matching approach [10] and the transverse resonance technique [11].

The formulation incorporating reflection matrices will be derived in Section II. The characteristic impedance of microshield lines with trapezoidal, circular, and V-shaped shields will be calculated to study the effects of the geometrical parameters such as strip width and gapwidth.

Manuscript received January 14, 1997; revised March 16, 1998. This work was supported by the National Science Council, Taiwan, R.O.C., under Contract NSC-86-2221-E005-011.

The author is with the Department of Electrical Engineering, National Chung-Hsing University, Taichung, Taiwan 402, R.O.C.

Publisher Item Identifier S 0018-9480(98)06153-5.

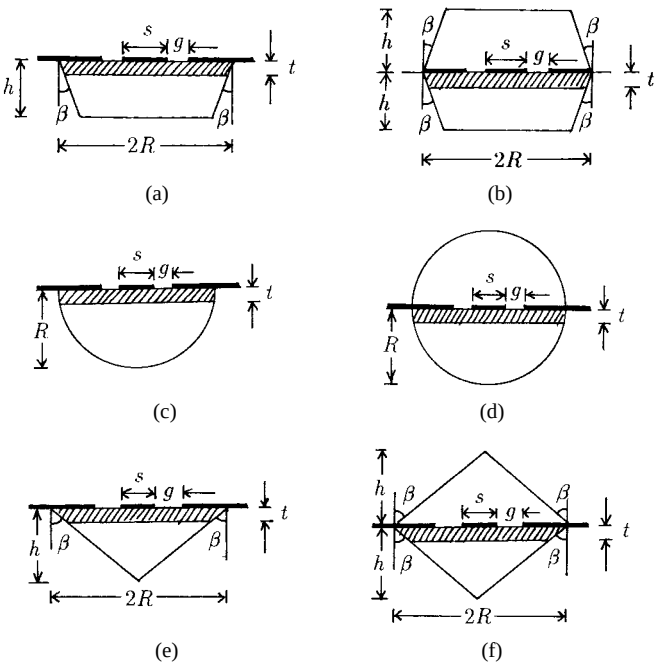

Fig. 1. Configuration of microshield lines with membrane. (a) Lower trapezoidal shield. (b) Complete trapezoidal shield. (c) Lower circular shield. (d) Complete circular shield. (e) Lower V-shaped shield. (f) Complete V-shaped shield. Hatching represents dielectric material.

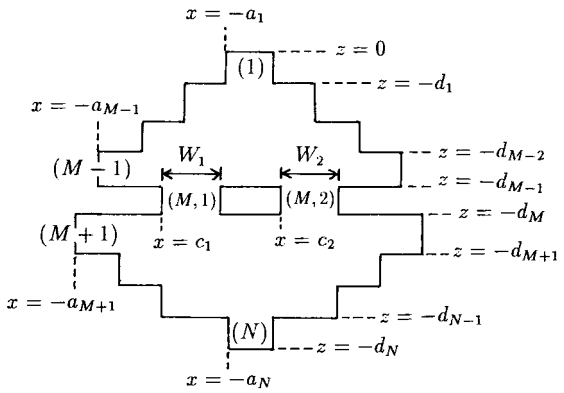

Fig. 2. Configuration of a microshield line modeled as layered media.

II. Formulation

Fig. 1 shows the configurations of three completely shielded microshield lines with membrane (CSML's/M) and three lower shielded microshield lines with membrane (LSML's/M). The trapezoidal, circular, and V-shaped shields are chosen for analysis. If the lower shield is filled with a dielectric, these microshield lines will be called CSML's and LSML's, to be differentiated from the versions with membrane. The shield itself forms part of the ground for the strip. The coplanar ground extended inside the shield are used to support the membrane mechanically. Thus, the microshield lines can be viewed as a coplanar waveguide enclosed by the shield. If the ground plane recedes out of the shield, the structure reduces to an enclosed microstrip lines.

As shown in Fig. 2, the CSML's can be modeled as a strip of finite thickness embedded in a layered medium where each layer has

a different width. If the boundary of the layered medium above the strip is expanded far away from the strip such that the upper shield walls have negligible effects on the strip, the structure approximates an LSML.

Assume that the microstrip line or coplanar waveguide is located in layer (M), the electric potential in layer (ℓ) can be expanded in terms of the harmonic functions, which are the solutions of the Laplace equation as

$$\Phi_\ell(\overline{r}) = \sum_{n=1}^{\infty} \sin[\gamma_{\ell n}(x+a_\ell)][\alpha_{\ell n} e^{-\gamma_{\ell n} z_\ell} + \beta_{\ell n} e^{\gamma_{\ell n} z_\ell}], \quad 1 \le \ell \le N,\ \ell \ne M$$

$$\Phi_{M,\lambda}(\overline{r}) = \sum_{n=1}^{\infty} \sin[\tau_{\lambda n}(x-c_\lambda)][\tilde{\alpha}_{\lambda n} e^{-\tau_{\lambda n} z_M} + \tilde{\beta}_{\lambda n} e^{\tau_{\lambda n} z_M}], \quad \lambda = 1,2 \tag{1}$$

where $z_\ell = z + d_\ell$ $(1 \le \ell \le N)$, $\gamma_{\ell n} = n\pi/b_\ell$ $(1 \le \ell \le N,\ \ell \ne M)$, $\tau_{\lambda n} = n\pi/W_\lambda$ $(\lambda = 1,2)$, b_ℓ is the width of layer (ℓ), and W_λ is the width of the λth gap.

For layers below layer (M), impose the conditions that the potential and normal electric-flux density are continuous at $z = -d_\ell$, then apply the orthogonality properties of the harmonic functions to obtain the recursive formula for the reflection matrices [12], [13]

$$\overline{\overline{R}}_{\cap\ell} = \left[\overline{\overline{S}}^{\ell(\ell+1)} \cdot \left(\hat{\overline{\overline{R}}}_{\cap(\ell+1)} + \overline{\overline{I}}\right) \cdot \left(\hat{\overline{\overline{R}}}_{\cap(\ell+1)} - \overline{\overline{I}}\right)^{-1} \cdot \overline{\overline{T}}^{(\ell+1)\ell} - \overline{\overline{I}}\right]^{-1} \cdot \left[\overline{\overline{S}}^{\ell(\ell+1)} \cdot \left(\hat{\overline{\overline{R}}}_{\cap(\ell+1)} + \overline{\overline{I}}\right) \cdot \left(\hat{\overline{\overline{R}}}_{\cap(\ell+1)} - \overline{\overline{I}}\right)^{-1} \cdot \overline{\overline{T}}^{(\ell+1)\ell} + \overline{\overline{I}}\right] \tag{2}$$

where the reflection matrix $\overline{\overline{R}}_{\cap\ell}$ at $z = -d_\ell$ is defined as $\overline{\alpha}_\ell = \overline{\overline{R}}_{\cap\ell} \cdot \overline{\beta}_\ell$, $\overline{\alpha}_\ell$ $(\overline{\beta}_\ell)$ is the vector consisting of the expansion coefficients $\{\alpha_{\ell n}\}$ $(\{\beta_{\ell n}\})$, and $\hat{\overline{\overline{R}}}_{\cap(\ell+1)} = \exp(-\overline{\overline{K}}_{\ell+1} h_{\ell+1}) \cdot \overline{\overline{R}}_{\cap(\ell+1)} \cdot \exp(-\overline{\overline{K}}_{\ell+1} h_{\ell+1})$ with $\overline{\overline{K}}_\ell = \mathrm{diag}\{\gamma_{\ell 1}, \gamma_{\ell 2}, \cdots\}$. Since $\Phi_N(\overline{r}) = 0$ at $z = -d_N$, we have $\overline{\overline{R}}_{\cap N} = -\overline{\overline{I}}$. The (m,n)th element of $\overline{\overline{S}}^{\ell(\ell+1)}$ and $\overline{\overline{T}}^{(\ell+1)\ell}$ are

$$S_{mn}^{\ell(\ell+1)} = \frac{2}{b_\ell} \int_{-a_{\ell+1}}^{-a_{\ell+1}+b_{\ell+1}} dx\ \sin[\gamma_{\ell m}(x+a_\ell)] \cdot \sin[\gamma_{(\ell+1)n}(x+a_{\ell+1})]$$

$$T_{mn}^{(\ell+1)\ell} = \frac{\epsilon_\ell \gamma_{\ell n}}{\epsilon_{\ell+1}\gamma_{(\ell+1)m}} \frac{2}{b_{\ell+1}} \int_{-a_{\ell+1}}^{-a_{\ell+1}+b_{\ell+1}} dx \cdot \sin[\gamma_{(\ell+1)m}(x+a_{\ell+1})] \sin[\gamma_{\ell n}(x+a_\ell)]. \tag{3}$$

Similarly, upward reflection matrices are defined for layers above layer (M), and a recursive formula is derived by matching the potential and normal electric-flux density at layer interfaces.

Next, impose the continuity condition of the potential and the normal electric-flux density at $z = -d_{M-1}$ and $z = -d_M$ to have

$$\begin{aligned} \overline{\overline{X}}_{11} \cdot \overline{\alpha} + \overline{\overline{X}}_{12} \cdot e^{\overline{\overline{K}}_M h_M} \cdot \overline{\beta} &= \overline{Y}_1 \\ \overline{\overline{X}}_{21} \cdot \overline{\alpha} + \overline{\overline{X}}_{22} \cdot e^{\overline{\overline{K}}_M h_M} \cdot \overline{\beta} &= \overline{Y}_2 \end{aligned} \tag{4}$$

where

$$\overline{\overline{X}}_{11} = \overline{\overline{Q}}_{M+1} \cdot \left(\hat{\overline{\overline{R}}}_{\cap(M+1)} - \overline{\overline{I}}\right) \cdot \left(\hat{\overline{\overline{R}}}_{\cap(M+1)} + \overline{\overline{I}}\right)^{-1} \cdot \overline{\overline{P}}_{M+1} - \overline{\overline{I}}$$

$$\overline{\overline{X}}_{12} = \left[\overline{\overline{Q}}_{M+1} \cdot \left(\hat{\overline{\overline{R}}}_{\cap(M+1)} - \overline{\overline{I}}\right) \cdot \left(\hat{\overline{\overline{R}}}_{\cap(M+1)} + \overline{\overline{I}}\right)^{-1} \cdot \overline{\overline{P}}_{M+1} + \overline{\overline{I}}\right] \cdot e^{-\overline{\overline{K}}_M h_M}$$

$$\overline{\overline{X}}_{21} = \left[\overline{\overline{Q}}_{M-1} \cdot \left(\overline{\overline{I}} - \hat{\overline{\overline{R}}}_{\cup(M-1)}\right) \cdot \left(\overline{\overline{I}} + \hat{\overline{\overline{R}}}_{\cup(M-1)}\right)^{-1} \cdot \overline{\overline{P}}_{M-1} - \overline{\overline{I}}\right] \cdot e^{-\overline{\overline{K}}_M h_M}$$

$$\overline{\overline{X}}_{22} = \overline{\overline{Q}}_{M-1} \cdot \left(\overline{\overline{I}} - \hat{\overline{\overline{R}}}_{\cup(M-1)}\right) \cdot \left(\overline{\overline{I}} + \hat{\overline{\overline{R}}}_{\cup(M-1)}\right)^{-1} \cdot \overline{\overline{P}}_{M-1} + \overline{\overline{I}}$$

$$\overline{Y}_1 = -\overline{\overline{Q}}_{M+1} \cdot \left(\hat{\overline{\overline{R}}}_{\cap(M+1)} - \overline{\overline{I}}\right) \cdot \left(\hat{\overline{\overline{R}}}_{\cap(M+1)} + \overline{\overline{I}}\right)^{-1} \cdot \overline{V}_{M+1}$$

$$\overline{Y}_2 = -\overline{\overline{Q}}_{M-1} \cdot \left(\overline{\overline{I}} - \hat{\overline{\overline{R}}}_{\cup(M-1)}\right) \cdot \left(\overline{\overline{I}} + \hat{\overline{\overline{R}}}_{\cup(M-1)}\right)^{-1} \cdot \overline{V}_{M-1}. \tag{5}$$

The parameters in (5) are listed in the Appendix.

Once the unknowns $\overline{\alpha}$ and $\overline{\beta}$ are obtained from (4), the total charge Q_t on the center strip can be calculated. The capacitance per unit length of the line is $C = Q_t/V_o$. The quasi-TEM analysis is then used to calculate the characteristic impedance as $Z_c = \sqrt{\mu_o \epsilon_o / C C_o}$ where C_o is the capacitance per unit length with all dielectrics replaced by vacuum.

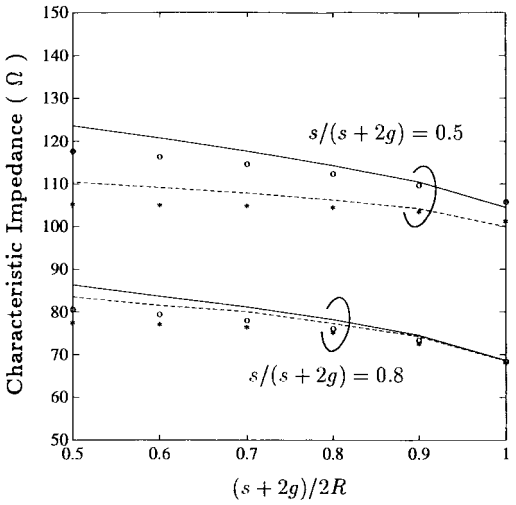

Fig. 3. Characteristic impedance of a microshield line with a rectangular shield (trapezoidal shield with $\beta = 0$), $\epsilon_m = \epsilon_o$. ———: this approach, $s/h = 0.2$, – – – –: this approach, $s/h = 1$, o: [5], $s/h = 0.2$, *: [5], $s/h = 1$.

III. Results and Discussions

Fig. 3 shows the characteristic impedance of an LSML with a rectangular shield (trapezoidal shield with $\beta = 0$), ϵ_m is the permittivity of the membrane. The results match reasonably well with those in [5]. The effect of gapwidth (indicated by the $s/(s+2g)$ parameter) is stronger than the distance between the strip and lower shield (indicated by the s/h parameter). This implies that the coplanar ground affects the impedance more significantly than the shield ground. Fig. 4 shows the effective dielectric constant of a CSML with a circular shield. Our results match reasonably well with those in [2], even at frequencies above the second higher order mode cutoff frequency.

In Fig. 5, we show the characteristic impedance of LSML's/M and CSML's/M with trapezoidal shields. Ten layers are used to approximate the trapezoidal cross section. One-hundred terms are used to expand the potential in the widest layer, and the numbers of terms used in the other layers are proportional to the layer width. Increasing either the number of layers or the number of expansion

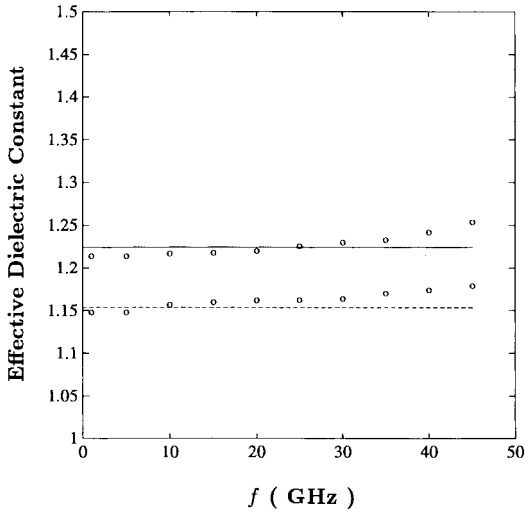

Fig. 4. Effective dielectric constant of a microshield line with a circular shield, $\epsilon_m = 2.22\epsilon_o$, $g = R - s/2$, $t = 0.08R$. ———: $s/R = 0.157$, – – – –: $s/R = 0.472$, o: results in [2].

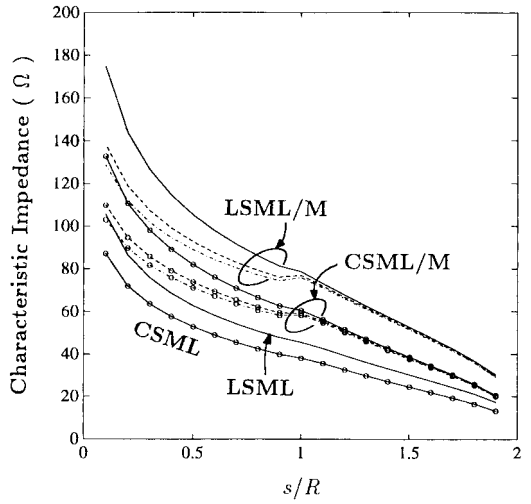

Fig. 5. Characteristic impedance of a microshield line with trapezoidal shields, $\epsilon_m = 4\epsilon_o$, $h = R/2$, $\beta = 45°$, $g = R - s/2$, ———: $t = 0.001R$, – – – –: $t = 0.01R$, – · – · –: $t = 0.02R$.

terms has a negligible effect on the charge distribution. It takes about 1 min to obtain the capacitance of one structure by using a Pentium PC. The same discretization scheme is applied to the other structures, and convergent results are always obtained.

As t approaches h, the LSML's/M and CSML's/M reduce to LSML's and CSML's, respectively. The characteristic impedance decreases with increasing membrane thickness. The impedance of the completely shielded lines is lower than that of the lower shielded lines because the electric field is more confined around the membrane in a CSML/M than in an LSML/M (hence, the capacitance of the former is larger than that of the latter). Increasing the strip width also increases the line capacitance; hence, reducing the characteristic impedance.

Around $s/R = 1$, the characteristic impedance increases slightly with increasing strip width. As the strip width increases, the field between the strip and sidewalls becomes stronger than that between the strip and bottom wall. Hence, there is a slight decrease of line capacitance. The membrane with higher dielectric constant further enhances this effect. As the strip width goes beyond $s/R = 1$, the field between the strip and sidewalls dominates, and further increase of strip width increases the capacitance. At $t = h$, the guidance effect of the membrane in favor of the sidewalls no longer exists. Thus, increasing the strip width increases the line capacitance and reduces the characteristic impedance.

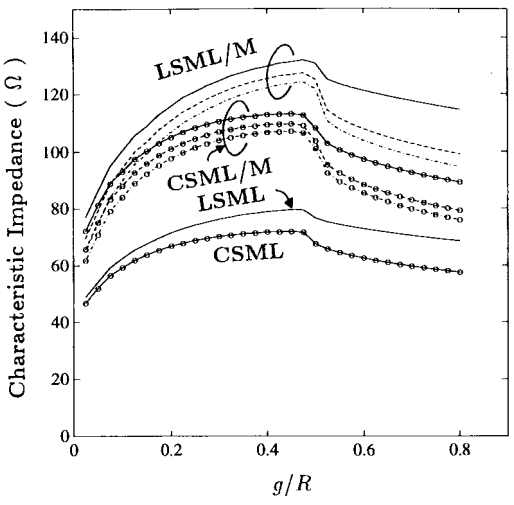

Fig. 6. Characteristic impedance of a microshield line with trapezoidal shields, $\epsilon_m = 4\epsilon_o$, $h = R/2$, $\beta = 45°$, $s = 0.4R$, ———: $t = 0.001R$, – – – –: $t = 0.01R$, – · – · –: $t = 0.02R$.

The characteristic impedance of microshield lines with a circular shield is also calculated. The reverse trend of impedance variation versus strip width around $s/R = 1$ is more obvious than the previous case because the bottom wall is farther away from the strip than in the previous case. Similar observation can also be found in the impedances curves with a V-shaped shield.

Next, analyze the effect of gapwidth on the characteristic impedance of microshield lines. In Fig. 6, we show the impedance of the LSML/M and CSML/M with trapezoidal shields. The gapwidth between the strip edge and coplanar ground is varied to study its effect. At small gapwidths, the electric field between the strip and the coplanar ground is stronger than that between the strip and bottom ground. Increasing gapwidth reduces the field around the gap; hence, the capacitance decreases and impedance increases. Around $g/R = 0.5$, the field lines starts to detach from the coplanar ground and attach to the bottom ground. As the gapwidth continue to increase, more field lines are released from the coplanar ground to the bottom ground. Hence, the capacitance increases and the impedance decreases. Since the CSML/M has a higher capacitance than the LSML/M does, the impedance of the CSML/M is lower than that of the LSML/M.

The variations of characteristic impedance versus gapwidth with circular and V-shaped shields are similar to those with the trapezoidal shield.

IV. Conclusion

We have developed a generalized potential-matching technique to calculate the capacitance and characteristic impedance of microshield lines enclosed by shields of arbitrary shape. Reflection matrices are defined to obtain a systematic formulation. Both lower shielded and completely shielded lines are analyzed, and the trapezoidal, circular, and V-shaped shields are considered. The effects of strip width and gapwidth between the strip and coplanar ground have been studied. The relative position of coplanar and shield grounds affects the dominant region of field distribution, thus determine the trend of characteristic impedance variation.

APPENDIX

The parameters appearing in (5) are

$$\begin{aligned}
\overline{\tilde{\alpha}} &= \begin{bmatrix} \overline{\tilde{\alpha}}_1 \\ \overline{\tilde{\alpha}}_2 \end{bmatrix} \\
\overline{\tilde{\beta}} &= \begin{bmatrix} \overline{\tilde{\beta}}_1 \\ \overline{\tilde{\beta}}_2 \end{bmatrix} \\
\overline{\overline{K}}_M &= \begin{bmatrix} \overline{\overline{K}}_{M,1} & 0 \\ 0 & \overline{\overline{K}}_{M,2} \end{bmatrix} \\
\overline{\overline{P}}_{M-1} &= [\overline{\overline{P}}_{(M-1),1} \quad \overline{\overline{P}}_{(M-1),2}] \\
\overline{\overline{Q}}_{M-1} &= \begin{bmatrix} \overline{\overline{Q}}_{(M-1),1} \\ \overline{\overline{Q}}_{(M-1),2} \end{bmatrix}.
\end{aligned} \tag{6}$$

The (m,n)th element of $\overline{\overline{P}}_{(M-1)\lambda}$ $(P_{(M-1)\lambda,mn})$, the (m,n)th element of $\overline{\overline{Q}}_{(M-1)\lambda}$ $(Q_{(M-1)\lambda,mn})$, and the mth element of $\overline{V}_{M-1}$ $(V_{M-1,m})$ are defined as

$$\begin{aligned}
P_{(M-1)\lambda,mn} &= \frac{2}{b_{M-1}} \int_{c_\lambda}^{c_\lambda+W_\lambda} dx \cdot \sin[\gamma_{(M-1)m}(x+a_{M-1})] \\
&\quad \cdot \sin[\tau_{\lambda n}(x-c_\lambda)] \\
Q_{(M-1)\lambda,mn} &= \frac{2\epsilon_{M-1}\gamma_{(M-1)n}}{W_\lambda \epsilon_M \tau_{\lambda m}} \int_{c_\lambda}^{c_\lambda+W_\lambda} dx \cdot \sin[\tau_{\lambda m}(x-c_\lambda)] \\
&\quad \cdot \sin[\gamma_{(M-1)n}(x+a_{M-1})] \\
V_{M-1,m} &= V_o \frac{2}{b_{M-1}} \int_{c_1+W_1}^{c_2} dx \cdot \sin[\gamma_{(M-1)m}(x+a_{M-1})].
\end{aligned} \tag{7}$$

The $\overline{\overline{P}}_{(M+1)\lambda}$, $\overline{\overline{Q}}_{(M+1)\lambda}$, and $\overline{V}_{M+1}$ are defined in a similar way. $\overline{\tilde{\alpha}}_\lambda$ $(\overline{\tilde{\beta}}_\lambda)$ is the vector consists of $[\tilde{\alpha}_{\lambda 1}, \tilde{\alpha}_{\lambda 2}, \cdots]$ $([\tilde{\beta}_{\lambda 1}, \tilde{\beta}_{\lambda 2}, \cdots])$.

ACKNOWLEDGMENT

The author would like to thank the reviewers for their useful comments.

REFERENCES

[1] T. M. Weller, L. P. B. Katehi, and G. M. Rebeiz, "High performance microshield line components," *IEEE Trans. Microwave Theory Tech.*, vol. 43, pp. 534–543, Mar. 1995.

[2] K. Wu and R. Vahldieck, "The method of lines applied to planar transmission lines in circular and elliptical waveguides," *IEEE Trans. Microwave Theory Tech.*, vol. 37, pp. 1958–1963, Dec. 1989.

[3] F. Medina and M. Horno, "Capacitance and inductance matrices for multistrip structures in multilayered anisotropic dielectrics," *IEEE Trans. Microwave Theory Tech.*, vol. MTT-35, pp. 1002–1008, Nov. 1987.

[4] K.-K. M. Cheng and I. D. Robertson, "Simple and explicit formulas for the design and analysis of asymmetrical V-shaped microshield line," *IEEE Trans. Microwave Theory Tech.*, vol. 43, pp. 2501–2504, Oct. 1995.

[5] ——, "Quasi-TEM study of microshield lines with practical cavity sidewall profiles," *IEEE Trans. Microwave Theory Tech.*, vol. 43, pp. 2689–2694, Dec. 1995.

[6] N. Yuan, C. Ruan, and W. Lin, "Analytical analyses of V, elliptic, and circular-shaped microshield transmission lines," *IEEE Trans. Microwave Theory Tech.*, vol. 42, pp. 855–859, May 1994.

[7] F. Medina and M. Horno, "Spectral and variational analysis of generalized cylindrical and elliptical strip and microstrip lines," *IEEE Trans. Microwave Theory Tech.*, vol. 38, pp. 1287–1293, Sept. 1990.

[8] J. E. Schutt-Aine, "Static analysis of V transmission lines," *IEEE Trans. Microwave Theory Tech.*, vol. 40, pp. 659–664, Apr. 1992.

[9] C. Wei, R. F. Harrington, J. R. Mautz, and T. K. Sarkar, "Multiconductor transmission lines in multilayered dielectric media," *IEEE Trans. Microwave Theory Tech.*, vol. MTT-32, pp. 439–450, Apr. 1984.

[10] T. Itoh, ed., "*Numerical Techniques for Microwave and Millimeter-Wave Passive Structures*." New York: Wiley, 1989.

[11] J. Bornemann, "Scattering-type transverse resonance technique for the calculation of (M)MIC transmission line characteristics," *IEEE Trans. Microwave Theory Tech.*, vol. 39, pp. 2083–2088, Dec. 1991.

[12] J.-F. Kiang, "Capacitance of microstrip lines with inhomogeneous substrate," *IEEE Trans. Microwave Theory Tech.*, vol. 44, pp. 1703–1709, Oct. 1996.

[13] ——, "Quasi-TEM analysis of coplanar waveguides with an inhomogeneous semiconductor substrate," *IEEE Trans. Microwave Theory Tech.*, vol. 44, pp. 1586–1589, Sept. 1996.

Cutoff Frequencies of an Asymmetrically Loaded Cylindrical Waveguide

Tat Soon Yeo

***Abstract*—The cutoff characteristics of an asymmetrically loaded cylindrical waveguide are analyzed using the null-field method. The fields in the metallic waveguide and dielectric loading are expressed in their corresponding guided-wave modes. The addition theorem of the Bessel function is used to relate the fields across the air–dielectric boundary.**

***Index Terms*—Asymmetric loading, cylindrical waveguide.**

I. INTRODUCTION

The computation of the cutoff frequencies and propagation constants of a cylindrical waveguide asymmetrically loaded with a dielectric cylinder has been the subject of much investigations [1], [2]. These research efforts have previously been pioneered by antenna designers interested in synthesizing specific aperture field across a cylindrical radiator; hence, leading to a specific radiation pattern. Lately, the hybrid microwave-integrated-circuit designers interested in accurately modeling the dielectric resonator enclosed within a metallic box are also seriously looking into this problem.

The reported work are often based on the concept of field matching across the air–dielectric boundary. Rothwell *et al.* [1] have used the simple point-matching method, while Yeo [2] has used the method of the least-squares boundary residual. While the legitimacy of the former method has often been called into question [3], the latter is a minimization procedure that has not been shown to be able to lead to a guaranteed global minimum.

On the other hand, the convergence and uniqueness of the null-field method [4] have been well proven [5]–[8]. In 1982, Martin [8] stated categorically that, "we prove that the infinite system of null-field equations always has precisely one solution." In this paper, the null-field method is used to compute the cutoff frequencies of the asymmetrically loaded cylindrical waveguide for both the transverse-electric and transverse-magnetic modes.

As correctly pointed out by Kuttler [9], the cross-sectional geometry of a asymmetrically loaded cylindrical waveguide is not easily

Manuscript received October 21, 1996; revised March 9, 1998.

The author is with the Department of Electrical Engineering, National University of Singapore, Singapore 119260.

Publisher Item Identifier S 0018-9480(98)06154-7.